UC Irvine
UC Irvine Previously Published Works

Title

Dermatological feasibility of multimodal facial color imaging modality for cross-evaluation of facial actinic keratosis

Permalink

Journal

ISSN

Authors

Bae, Youngwoo
Son, Taeyoon
Nelson, J Stuart
et al.

Publication Date

DOI

Copyright Information

Peer reviewed

Dermatological Feasibility of Multimodal Facial Color Imaging Modality for Cross-Evaluation of Facial Actinic Keratosis

Youngwoo Bae, B.S.[1], **Taeyoon Son, M.S.**[1], **J. Stuart Nelson, M.D., Ph.D.**[2], **Jae-Hong Kim, M.D.**[3], **Eung Ho Choi, M.D.**[3,5], and **Byungjo Jung, Ph.D.**[*,1,4]

[1]Department of Biomedical Engineering, Yonsei University, Wonju, Korea

[2]Beckman Laser Institute, University of California, Irvine, CA, USA

[3]Department of Dermatology, Yonsei University Wonju College of Medicine, Wonju, Korea

[4]Institute of Medical Engineering Yonsei University, Wonju, Korea

[5]Yonsei Institute of Lifelong Health, Wonju, Korea

Abstract

Background/Purpose—Digital color image analysis is currently considered as a routine procedure in dermatology. In our previous study, a multimodal facial color imaging modality (MFCIM), which provides a conventional, parallel- and cross-polarization, and fluorescent color image, was introduced for objective evaluation of various facial skin lesions. This study introduces a commercial version of MFCIM, *DermaVision-PRO*, for routine clinical use in dermatology and demonstrates its dermatological feasibility for cross-evaluation of skin lesions.

Methods/Results—Sample images of subjects with actinic keratosis or non-melanoma skin cancers were obtained at four different imaging modes. Various image analysis methods were applied to cross-evaluate the skin lesion and, finally, extract valuable diagnostic information. *DermaVision-PRO* is potentially a useful tool as an objective macroscopic imaging modality for quick prescreening and cross-evaluation of facial skin lesions.

Conclusion—*DermaVision-PRO* may be utilized as a useful tool for cross-evaluation of widely distributed facial skin lesions and an efficient database management of patient information.

Keywords

DermaVision-PRO; Actinic keratosis; Cross-evaluation; Multimodal imaging

Introduction

Optical measurement of skin color can be categorized into two main modalities: spectrophotometric (such as, reflectance spectrophotometers) and tristimulus (such as, colorimeters) analysis (1). Even though such modalities hold great promise, it would be impractical and cumbersome in routine clinical use to evaluate every single skin lesion by using such point measurement-based techniques. Furthermore, they are limited in use by practical considerations, such as, difficulty to observe spatial pattern in skin lesions, potential skin blanching due to probe contact, and poor reproducibility of the measurement on identical skin lesions (1-3). Alternatively, a hyper-spectral imaging modality, which addresses the drawbacks of conventional imaging modalities, has been introduced to

[*]Corresponding Author: Byungjo Jung, Ph.D., Department of Biomedical Engineering, Yonsei University, 234 Maeji, Heungup-myun, Wonju-si, Gangwon-do, 220-710, Korea, Tel: +82 33 760 2786, Fax: +82 33 763 1953, bjung@yonsei.ac.kr.

evaluate abnormalities of skin lesions (4). However, it requires a relatively long image acquisition time (typically more than 30 sec for an image cube) which causes motion artifact during image acquisition. Therefore, it may not be an appropriate method for routine clinical use.

Digital color image analysis is currently considered as a routine clinical procedure because it is relatively convenient in the evaluation of skin lesions, minimizing unnecessary biopsies (5). However, conventional digital color image analysis has been qualitatively and subjectively conducted due to the lack of reproducibility of imaging conditions, such as, camera setup, optical lens system, patient positioning, and illumination (2,6). Furthermore, human visual assessment can be altered by physiological and psychological conditions even though the imaging conditions are controlled (7).

Recently, several articles have addressed such issues and introduced reproducible digital imaging modalities for quantitative and objective analysis of facial skin lesions (8-11). Even though the digital imaging modalities have provided valuable diagnostic information regarding facial skin lesions, they could not simultaneously differentiate and evaluate all the characteristics of various skin disorders and, therefore, might result in misdiagnosis due to the use of fragmented information. In this sense, it is indispensable to integrate independent digital imaging modalities into a multimodal imaging modality for the cross-evaluation of skin lesions in dermatology.

In our previous study, a prototype of a multimodal facial color imaging modality (MFCIM) was introduced, and sample images were analyzed for objective evaluation of facial skin lesions (6). It has four different imaging modes, such as, a conventional color image (CCI), parallel- and cross-polarization color images (PPCI and CPCI), and UV-A induced fluorescent color image (FCI). In addition, a polarization image (PI) derived from parallel- and cross-polarization color images may help to estimate the margins of facial skin lesion abnormalities (12,13). In this study, a commercial version of the MFCIM, *DermaVision-PRO*, was developed for routine clinical use in dermatology and its dermatological feasibility was investigated by cross-evaluating facial skin lesions, actinic keratosis (AK) and squamous cell carcinoma (SCC).

Materials and Method

Hardware of DermaVision-PRO

Figures 1(a) and (b) show the commercial version of MFCIM based on our previous study (6) and the schematic diagram of the imaging box, respectively. Four UV-A lamps (315 - 380 nm, BLACK LAMP 30 W, ALIM, Korea) and a flash white light embedded in a digital camera (Canon EOS 400D, Canon Inc., Tokyo, Japan) were employed as light sources. A linear polarizer (Model A45-669, Edmund Industrial Optics, Barrington, NJ) was placed in front of the digital camera lens. A three-position linear filter holder was equipped in front of the flash white light in order to produce linearly polarized light. Three linear polarizers were integrated into the filter holder at an angle of 45° (for CCI), 90° (for CPCI), and 0° (for PPCI) over the polarization direction of the linear polarizer in front of the digital camera lens. The digital camera was placed at the center of four UV-A lamps and operated at manual mode. A head-positioning device, which simultaneously supports the forehead and jaw and can be adjusted in both vertical and horizontal directions, was installed into the imaging box in order to ensure reproducible image acquisition (2). To minimize artifacts by ambient light, a blackout curtain frame was incorporated into the imaging box.

Software of DermaVision-PRO

Image analysis software of *DermaVision-PRO* was written with "Visual C++" and provides a graphic user interface (GUI). The software mainly consists of "Single Image Analysis Window" and "Total Image Analysis Window" with various image analysis tools, which have shown their clinical validity in previous studies (2,3,8,9-13).

The "Single Image Analysis Window" [Fig. 2(a)] provides a full-scale image for close-up investigation of original and processed images. The basic concept and clinical validity of image analysis for each image mode were well demonstrated in our previous study (6). The basic function of "Total Image Analysis Window" [Fig. 2(b)] is to compare the images of skin lesions before and after treatment. In order to evaluate the treatment result more efficiently, the clinician can cross-evaluate facial skin lesions by comparing their subjective evaluation to quantitative information derived from different image modes.

Clinical Trials

Facial skin abnormalities, such as, facial actinic (solar) keratosis (AK) and non-melanoma skin cancer (NMSC), were evaluated in order to demonstrate the dermatological feasibility of *DermaVision-PRO* as a pre-screening and cross-evaluation tool. Fourteen Asians [AK: 11 subjects, and squamous cell carcinoma (SCC): 3 subjects] were recruited and images taken at four different imaging modes and processed. Before the image acquisition, subjects were classified according to medical examinations by dermatologists at the Department of Dermatology, Yonsei University. In order to verify the medical examinations, tissue specimens were extracted from the skin lesions, using a 2 mm biopsy punch, and preserved in 10% formalin solution for Hematoxylin and Eosin staining.

Results

Subjects with AK and SCC lesions may present endogenous fluorescent signal [Fig. 3(c)] or not [Fig. 4(c)] for UVA (320 - 380 nm) excitation, depending on the severity of the skin lesions. Eleven out of 14 subjects presented the endogenous fluorescent signals with various intensities and three did not present. The identical region was quantitatively analyzed by computing the melanin index (M.I.) [Figs. 3(a) and 4(a)] and erythema index (E.I.) [Figs. 3(b) and 4(b)] images, which are useful for the evaluation of pigmented and vascular skin lesions, respectively (6, 8). Higher index values indicate higher melanin and erythema content. All eleven (three) subjects with (without) endogenous fluorescent signals presented relatively higher (lower) E.I. at the surrounding normal skin region than the AK and SCC lesions.

The fluorescent intensity and E.I. at the surrounding normal skin region and AK lesions were computed across all eleven subjects with endogenous fluorescence [Fig. 5]. Five different points from FCI and E.I. images were randomly selected from AK lesions and the surrounding normal skin region, and their mean values were computed. The fluorescent intensity on the AK lesion (FLlesion: 200.57 ± 42.82) was 1.84 times higher than the surrounding normal skin region (FLnormal: 108.50 ± 36.85). The E.I. on the surrounding normal skin region (E.I.normal: 27.13 ± 6.22) was 3.51 times higher than the AK lesion (E.I.lesion: 7.71 ± 5.27).

It is difficult to observe morphological features of the skin lesions because of non-uniform distribution of the melanin in the region of interest (ROI) [Figs. 3(a) and 4(a)]. Such an issue was addressed by computing the PI, which provides a contrast enhanced image of superficial skin layers where skin cancer often arises as well as of the texture of the dermis (papillary and upper reticular dermis) while eliminating the melanin effect in the epidermis [Figs. 3(d) and 4(d)] (12, 13).

Discussion

AK is considered as a precancerous skin lesion that results from the loss of orderly maturation of atypical keratinocytes (14). Clinically, it presents ill-defined macule, papule or plaque-like features, and a skin color of reddish brown or yellowish black (14,15). Because of its distinctive surface texture, it is often recognized by palpation rather than visualization. However, it is occasionally not well recognized with other skin abnormalities, such as, seborrheic keratoses, porokeratoses, viral warts, superficial basal cell carcinoma (BCC), and allergic and contact dermatitis, as well as often associated with other sun-damaged skin lesions, such as, solar lentigo, telangiectasia, and solar elastosis (16-18). Also, it is sometimes considered to be a potential precursor lesion of SCC (14-18). Therefore, it may be useful for clinicians to recognize visually and non-invasively specific features of AK in order to minimize the number of unnecessary histopathologic examinations.

Four different images of an identical facial skin lesion [yellow dotted line in Figs. 3 and 4] were obtained in order to cross-evaluate visually specific features of AK. Similar to clinical examination by the naked eye, CCI provides both surface and subsurface morphological features of skin lesions, simultaneously. It is difficult to discern the AK lesions from the surrounding normal skin region because the property of superficially backscattered light from the AK itself is lost by the superposition of backscattered light from the dermis, and hyperpigmentation on the AK lesion absorbs most of the incident and backscattered light.

FCI [Fig. 3(c)] provides an endogenous fluorescent characteristic of the AK skin lesion. According to previous studies, the fluorescent method has been mainly used in the diagnosis of some infective, pigmentary dermatoses and keratosis (23, 24). The fluorescence signals are mainly caused by tissue fluorophores, such as, elastin, collagen, aromatic amino acids, and nicotinamide adenine dinucleotide (NAD) in abnormal skin lesions (19, 23).

Consequently, FCI provides additional fluorescent properties in abnormal skin lesions which are difficult to recognize with reflectance imaging methods, such as, CCI, PPCI, and CPCI. As shown, the AK lesion demonstrated significantly higher endogenous fluorescent intensity [white dotted line in Fig. 3(c)] than the surrounding normal (hyperpigmented) skin regions which showed mild (lower) endogenous fluorescence intensity. In this study, we assume that only two fluorophores of a reduced nicotinamide adenine dinucleotide (NADH) with emission peaks at 420 and 460 nm and porphyrin with emission peaks at 630 and 690 nm are mainly attributed to relatively higher fluorescent intensity of AK and SCC because: 1) the spectral range of the UV light source and digital camera covers only 320-380 nm for excitation and 400-700 nm for emission (candidate fluorophores: collagen, elastin, porphyrins, and NADH), respectively (19); 2) in the spectral range, it has been reported that two such fluorophores present dynamic changes of fluorescence intensity during neoplastic transformation (20). According to *Wollina et al.* (18), NADH on AK lesions excited at 370 nm resulted in the increase of fluorescence signal at the emission wavelength peaks of 430 and 470 nm in a human *in-vivo* study. It has been reported that the increased metabolic activity during the dysplasia/hyperplasia process, especially AK, can be recognized by an increased NADH fluorescent emission signal (20 - 22). Furthermore, porphyrin, which is dynamically changed during the neoplastic sequence, has been reported from inflamed cells on the skin surface and necrotic tumor surface (20).

The M.I. [Figs. 3(a) and 4(a)] derived from CPCI represents the degree of skin pigmentation (melanin content) (6, 8). Although the M.I. itself might be a valuable objective parameter for melanin content, especially in the case of pigmented AK, we confirmed that the M.I. could not be used alone as a criteria for the evaluation of AK lesions because AK can be categorized into at least five classes according to different clinical features (14, 17).

Different from M.I., which is randomly distributed in the ROI, E.I. presents a relatively higher value on the surrounding normal skin region in the fluorescent group [Fig. 3(b)], and on the AK skin lesions in the non-fluorescent group [Fig. 4 (b)]. The thickening of the tissues (epithelial cell layer) and vasculature formation during the middle stage of AK may lead to reduced NADH fluorescent emission signal in the non-fluorescent group [Fig. 4(c)] because the emission peak of NADH fluorescence exists near the absorption peak of hemoglobin (19). On the other hand, the rapid cell proliferation during the initial stage of AK and after the differentiation to SCC may lead to increasing the NADH fluorescence intensity at the fluorescent group [Fig. 3(c)] (21, 22).

Figures 3(d) and 4(d) show the PI in the ROI. As shown, a freckle is apparent in other image modes, but the melanin has been eliminated in the PI [white solid line in Fig. 3(d)] such that it gives a chance for clinicians to examine non-invasively the morphology of relatively deep skin layers. Besides, it is remarkable that the margin of AK defined by the PI is relatively wider and more apparent than that defined by the FCI. Although it is difficult to conclude which one is the real margin of the AK, it seems that the PI can be utilized as a criterion to estimate morphological characteristics of dermatological abnormalities (for example, non-melanoma skin cancers, such as, BCC and SCC, which most frequently occur in the superficial skin layer).

Overall, the different fluorescence intensity of NADH and porphyrin among subjects with facial AK may be interpreted as different phases of morphological and metabolic changes during the tissue transformation process of AK as it is partially demonstrated with E.I.. Besides, all three subjects with facial SCC presented relatively higher fluorescence intensity on the skin lesion and the fluorescence pattern was analogous to previous studies (20,21). We can elucidate from the results that *DermaVision-PRO* may be utilized for cross-evaluation of facial AK and SCC lesions so that it should be a quick prescreening tool for routine clinical use in dermatology even though it does not completely substitute for histopathological examinations.

Conclusion

A commercial version of a MFCIM, *DermaVision-PRO*, was developed for routine clinical use in dermatology. It demonstrated dermatological feasibility as a macroscopic prescreening imaging modality for cross-evaluation of facial skin lesions, such as, AK and SCC. We are confident that *DermaVision-PRO* may be utilized as a useful prescreening tool for widely distributed facial skin lesions and as an efficient database management of patient information.

Acknowledgments

References

1. Fullerton A, Fischer T, Lahti A, et al. Guidelines for measurement of skin colour and erythema. A report from the Standardization Group of the European Society of Contact Dermatitis. Contact Dermatitis. 1996; 35:1–10. [PubMed: 8896947]

2. Jung B, Choi B, Shin Y, et al. Determination of optimal view angles for quantitative facial image analysis. J Biomed Opt. 2005; 10:024002. [PubMed: 15910076]

3. Jung B, Kim CS, Choi B, et al. Use of erythema index imaging for systematic analysis of port wine stain skin response to laser therapy. Lasers Surg Med. 2005; 37:186–91. [PubMed: 16175634]
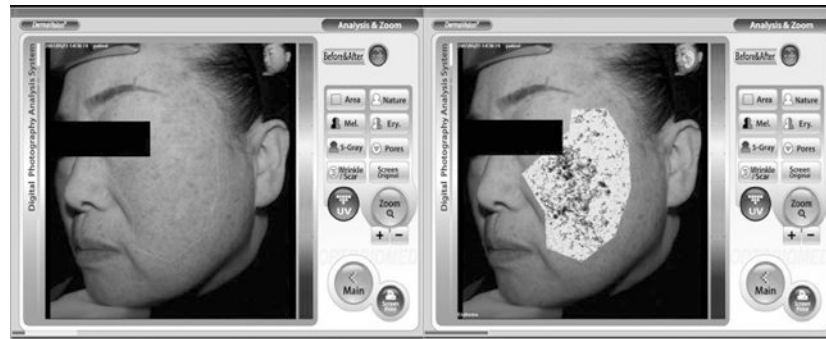
4. Wallace VP, Crawford DC, Mortimer PS, et al. Spectrophotometric assessment of pigmented skin lesions: methods and feature selection for evaluation of diagnostic performance. Phys Med Biol. 2000; 45:735–51. [PubMed: 10730968]

5. Marghoob AA, Swindle LD, Moricz CZ, et al. Instruments and new technologies for the in vivo diagnosis of melanoma. J Am Acad Dermatol. 2003; 49:777–97. quiz 98-9. [PubMed: 14576657]

6. Bae Y, Nelson JS, Jung B. Multimodal facial color imaging modality for objective analysis of skin lesions. J Biomed Opt. 2008; 13:064007. [PubMed: 19123654]

7. Yong-Gee SA, Kurwa HA, Barlow RJ. Objective assessment of port-wine stains following treatment with the 585 nm pulsed dye laser. Australas J Dermatol. 2001; 42:243–6. [PubMed: 11903154]

8. Kang H, Jung B, Nelson JS. Polarization color imaging system for on-line quantitative evaluation of facial skin lesions. Dermatol Surg. 2007; 33:1350–6. [PubMed: 17958588]

9. Jung B, Kim CS, Choi B, et al. Use of erythema index imaging for systematic analysis of port wine stain skin response to laser therapy. Lasers Surg Med. 2005; 37:186–91. [PubMed: 16175634]

10. Muccini JA, Kollias N, Phillips SB, et al. Polarized light photography in the evaluation of photoaging. J Am Acad Dermatol. 1995; 33:765–9. [PubMed: 7593775]

11. Han B, Jung B, Nelson JS, et al. Analysis of facial sebum distribution using a digital fluorescent imaging system. J Biomed Opt. 2007; 12:014006. [PubMed: 17343481]

12. Jacques SL, Ramella-Roman JC, Lee K. Imaging skin pathology with polarized light. J Biomed Opt. 2002; 7:329–40. [PubMed: 12175282]

13. Jacques SL, Roman JR, Lee K. Imaging superficial tissues with polarized light. Lasers Surg Med. 2000; 26:119–29. [PubMed: 10685085]

14. Roewert-Huber J, Stockfleth E, Kerl H. Pathology and pathobiology of actinic (solar) keratosis - an update. Br J Dermatol. 2007; 157(Suppl 2):18–20. [PubMed: 18067626]

15. Schwartz RA, Bridges TM, Butani AK, et al. Actinic keratosis: an occupational and environmental disorder. J Eur Acad Dermatol Venereol. 2008; 22:606–15. [PubMed: 18410618]

16. Horn M, Gerger A, Ahlgrimm-Siess V, et al. Discrimination of actinic keratoses from normal skin with reflectance mode confocal microscopy. Dermatol Surg. 2008; 34:620–5. [PubMed: 18429925]

17. Peris K, Micantonio T, Piccolo D, et al. Dermoscopic features of actinic keratosis. J Dtsch Dermatol Ges. 2007; 5:970–6. [PubMed: 17908179]

18. Wollina U, Nelskamp C, Scheibe A, et al. Fluorescence-remission sensoring of skin tumours: preliminary results. Skin Res Technol. 2007; 13:463–71. [PubMed: 17908200]

19. Ramanujam N. Fluorescence spectroscopy of neoplastic and non-neoplastic tissues. Neoplasia. 2000; 2(1-2):89–117. [PubMed: 10933071]

20. Diagaradjane P, Yaseen MA, Yu J, Wong MS, Anvari B. Autofluorescence characterization for the early diagnosis of neoplastic changes in DMBA/TPA-induced mouse skin carcinogenesis. Lasers Surg Med. 2005; 37(5):382–95. [PubMed: 16240416]

21. Mayevsky A, Chance B. Intracellular oxidation-reduction state measured in situ by a multichannel fiber-optic surface fluorometer. Science. 1982; 217(4559):537–40. [PubMed: 7201167]

22. Varani J, Hattori Y, Chi Y, Schmidt T, Perone P, Zeigler ME, et al. Collagenolytic and gelatinolytic matrix metalloproteinases and their inhibitors in basal cell carcinoma of skin: comparison with normal skin. Br J Cancer. 2000; 82(3):657–65. [PubMed: 10682680]

23. Asawanonda P, Taylor CR. Wood's light in dermatology. Int J Dermatol. 1999; 38:801–7. [PubMed: 10583611]

24. Niamtu J 3rd. Digitally processed ultraviolet images: a convenient, affordable, reproducible means of illustrating ultraviolet clinical examination. Dermatol Surg. 2001; 27:1039–42. [PubMed: 11849267]
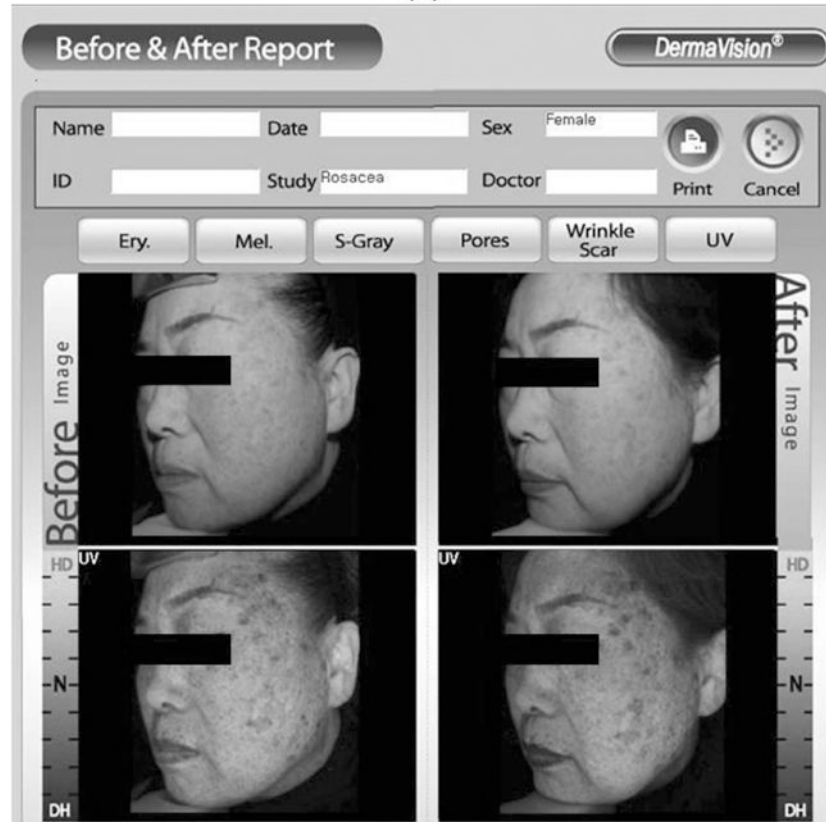
Figure 1.
(a) *DermaVision-PRO* consists of an imaging box (1), display panel (2), and software control panel (3). (b) The imaging box consists of a flash white light (4), a digital color camera (5), three-position linear polarizer holder (6), and four UV-A lamps (7). Linearly polarized light (8) and UV-A radiation (9) incident to human face on head-positioning device (10) are reflected back to the digital color camera.
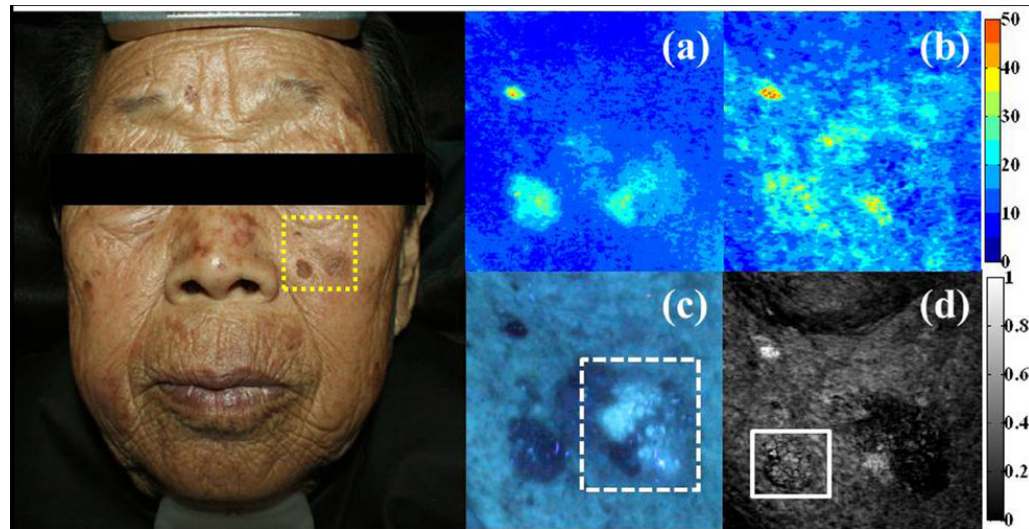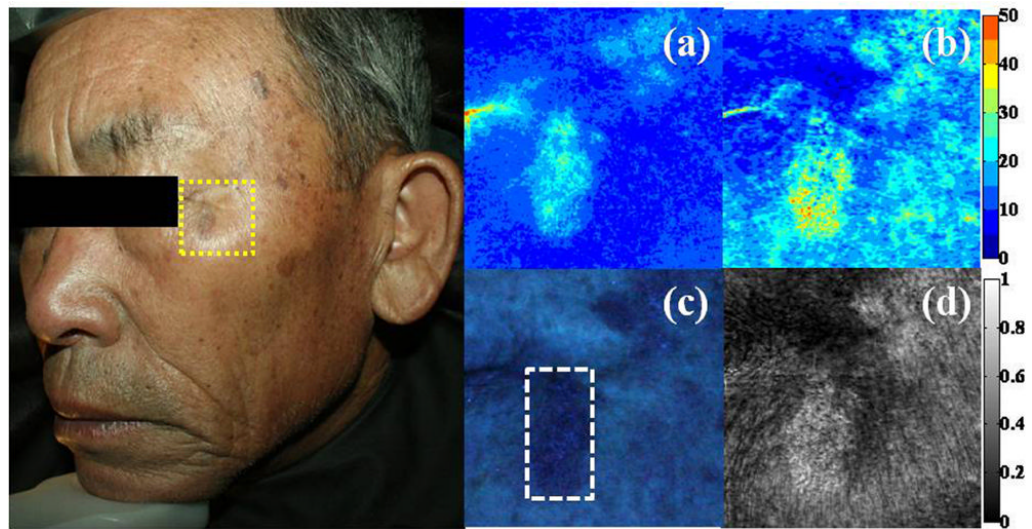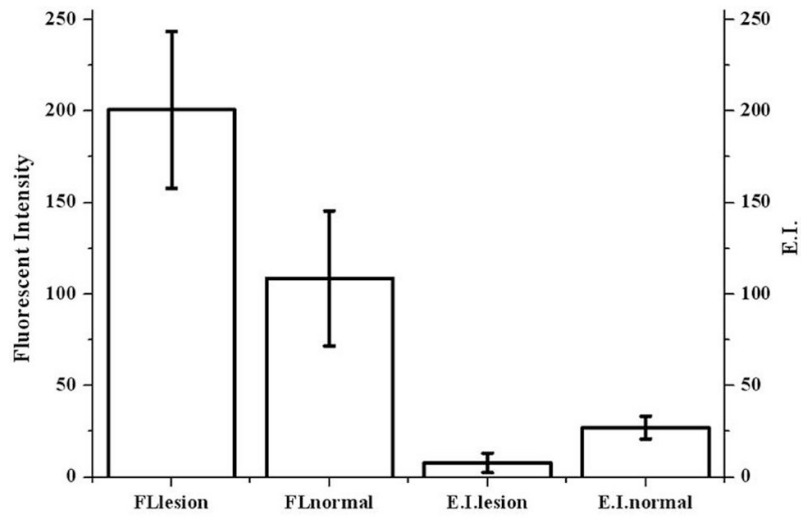
(a)

(b)

Figure 2.
(a) "Single Image Analysis Window" provides a full-scale image for close-up investigation of processed images which stem from different image channels. (b) "Total Image Analysis Window" provides comparison of images before and after treatment.

Figure 3.
Multimodal images of a female subject with fluorescent actinic (solar) keratosis (AK) on facial skin lesions: (a) melanin index image; (b) erythma index image computed from CPCI; (c) fluorescent color image (FCI); (d) polarization image (PI).

Figure 4.
Multimodal images of a male subject with non-fluorescent actinic (solar) keratosis (AK) on facial skin lesions: (a) melanin index image; (b) erythma index image computed from CPCI; (c) fluorescent color image (FCI); (d) polarization image (PI).

Figure 5.
Comparison of the fluorescent intensity and E.I. on AK lesions and surrounding normal skin regions in the fluorescent group.